THE UNIVERSITY *of* EDINBURGH

Edinburgh Research Explorer

Maturation of AMPAR Composition and the GABAAR Reversal Potential in hPSC-Derived Cortical Neurons

OPEN ACCESS

Brief Communications

Maturation of AMPAR Composition and the GABA$_A$R Reversal Potential in hPSC-Derived Cortical Neurons

Matthew R. Livesey,[1,2,3]* **Bilada Bilican,**[2,3,4]* **Jing Qiu,**[1] **Nina M. Rzechorzek,**[2,3,4] **Ghazal Haghi,**[1,2,3] **Karen Burr,**[2,3,4] **Giles E. Hardingham,**[1] **Siddharthan Chandran,**[2,3,4] **and David J.A. Wyllie**[1]

[1]Centre for Integrative Physiology, University of Edinburgh, Edinburgh EH8 9XD, United Kingdom; and [2]Euan MacDonald Centre for MND Research, [3]Centre for Clinical Brain Sciences, and [4]MRC Centre for Regenerative Medicine, University of Edinburgh, Edinburgh EH16 4SB, United Kingdom

Rodent-based studies have shown that neurons undergo major developmental changes to ion channel expression and ionic gradients that determine their excitation-inhibition balance. Neurons derived from human pluripotent stem cells theoretically offer the potential to study classical developmental processes in a human-relevant system, although this is currently not well explored. Here, we show that excitatory cortical-patterned neurons derived from multiple human pluripotent stem cell lines exhibit native-like maturation changes in AMPAR composition such that there is an increase in the expression of GluA2(R) subunits. Moreover, we observe a dynamic shift in intracellular Cl$^-$ levels, which determines the reversal potential of GABA$_A$R-mediated currents and is influenced by neurotrophic factors. The shift is concomitant with changes in KCC2 and NKCC1 expression. Because some human diseases are thought to involve perturbations to AMPAR GluA2 content and others in the chloride reversal potential, human stem-cell-derived neurons represent a valuable tool for studying these fundamental properties.

Key words: GABA; glutamate; neurotransmitter; patch clamp; qRT-PCR; stem cells

Introduction

The ability to generate *in vitro* cortical neuronal populations from human pluripotent stem cells (hPSCs) provides an experimental resource for the investigation of human cortical physiology and disease (Hansen et al., 2011). hPSCs have been used to derive human excitatory cortical neurons (hECNs) *in vitro* that appear to recapitulate aspects of *in vivo* cortical development (Johnson et al., 2007; Zeng et al., 2010; Shi et al., 2012; Espuny-Camacho et al., 2013). We have developed a protocol that enables the generation of a propagatable pool of anterior neural precursor cells (aNPCs) from human embryonic stem (ES) cell and induced pluripotent stem cell lines (Bilican et al., 2014). aNPCs can be efficiently differentiated as a monolayer of excitatory cortical neurons that are representative of neuronal populations present within native upper and lower cortical layers. Our recent study (Bilican et al., 2014) demonstrated the ability of hECNs to fire action potentials, express voltage-gated and ligand-gated ion channels, and exhibit putative synaptic activity; however, there is a need to identify specific physiologically postnatal/adult properties of such neurons to aid *in vitro* human studies of neurodevelopmental physiology and modeling of neurodevelopmental and adult diseases (Yang et al., 2011; Sandoe and Eggan, 2013).

Here, we demonstrate that hECNs differentiated from aNPCs exhibit native-like maturation shifts in AMPAR subunit composition and in the relative expression of the Na$^+$-K$^+$-Cl$^-$ cotransporter-1 (NKCC1) and K$^+$-Cl$^-$ cotransporter-2 (KCC2) subunits to reduce intracellular chloride concentration ([Cl$^-$]$_{INT}$), which determine the nature of GABA receptor type-A (GABA$_A$R) function (Blaesse et al., 2009). Beyond a platform for the study of maturation, these hECNs are of interest for studies of human diseases in which AMPAR and [Cl$^-$]$_{INT}$ regulation are disrupted (Blaesse et al., 2009; Wright and Vissel, 2012).

Materials and Methods

In vitro hECN preparation. A detailed description of the derivation of hECNs, including immunohistochemistry protocols, can be found in Bilican et al. (2014) and is summarized in Figure 1A. The H9 (female), hereafter referred to as ES1 (WiCell) and SHEF4 (male), referred to as ES2 (UK Stem Cell Bank) human ES cell lines were obtained under full ethical/Institutional Review Board approval of the University of Edinburgh. For IPS1 (male M337V mutant line 1; Bilican et al., 2012) and IPS2 (female in-house control line) human IPS cell lines, written informed consent was obtained from each participant.

hECN culture media supplements. Forskolin (10 μM) was present during weeks 1–3 of differentiation. For AMPAR characterization, medium was supplemented with BDNF and GDNF (both 5 ng/ml) from week 3 onward. For experiments to determine [Cl$^-$]$_{INT}$, BDNF and GDNF were omitted unless otherwise stated. When cultures were maintained beyond 5 weeks, the culture medium was supplemented with IGF1 (10 ng/ml) from week 4 of differentiation.
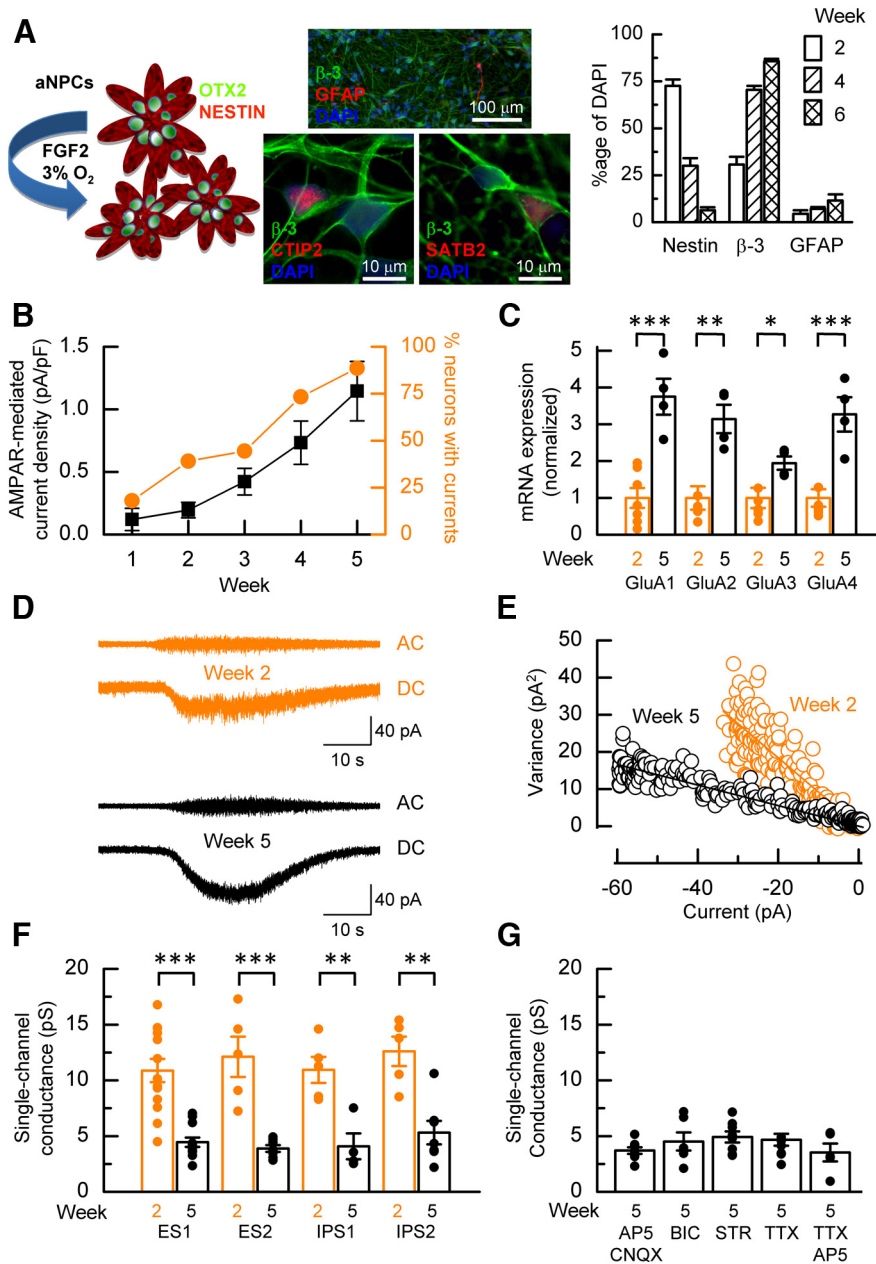
Figure 1. AMPAR maturation. **A**, Schematic representation of hECNs derived from OTX2^{+} and Nestin[+] aNPCs. Neuronal differentiation is initiated by the removal of FGF2 and cultures are maintained in a 3% O_2 atmosphere (Bilican et al., 2014). Immunocytochemistry for neuronal (β3-tubulin) astrocyte (glial fibrillary acidic protein; GFAP) and aNPC (Nestin) markers indicates increasing neuronal differentiation with time in culture and sparse astrocytes throughout. Bar graph displays cell marker counts as a percentage of DAPI-stained nuclei. hECNs are also immunopositive for deep and superficial cortical layer markers CTIP2 and SATB2, respectively. **B**, Weekly percentage response (orange) to AMPA and the mean AMPA-mediated current density (black). $n = 22$–35, $N > 3$. **C**, Mean normalized mRNA fold expression data for AMPAR subunits GluA1-GluA4 in week 2 and 5 cells as assessed by qRT-PCR. $n = 4$–6, $N = 3$, unpaired t test. Relative expression of each subunit of one of the week 2 samples is set to 1 after normalizing to β-actin. **D**, Example nonstationary fluctuation analysis of AMPAR-mediated whole-cell currents from a week 2 (orange) and 5 (black) neurons. **E**, Plot of the relationship between the variance of the AC-coupled current and DC-current amplitude for the respective recordings of week 2 (orange) and week 5 neurons (black) shown in **D**. Linear regression analysis of the relationships for week 2 and 5 data gave respective unitary single-channel current amplitude estimates of -1 pA and -0.3 pA from which the unitary conductance was calculated. **F**, A decrease in mean conductance is observed in other hPSC lines. $n = 4$–13, $N = 1$–3, unpaired t test. **G**, The switch to lower conductance AMPARs was not prevented by antagonists. $n = 5$–9, $N = 1$–2, one-way ANOVA with *post hoc* Tukey's test.

Electrophysiology. Whole-cell patch-clamp recordings were made from hECNs using an Axon Multiclamp 700B amplifier (Molecular Devices). AMPA-evoked currents were made at a holding potential of -74 mV in the presence of picrotoxin (50 μM), strychnine (20 μM), and TTX (300 nM). GABA-evoked currents were made at a holding potential of -14 mV in the presence of CNQX (5 μM), D-APV (50 μM), strychnine, and TTX. Patch electrodes were filled with a solution containing the following (in mM): 155 K-gluconate, 2 MgCl$_2$, 10 Na-HEPES, 10 Na-PiCreatine, 2 Mg$_2$-ATP, and 0.3 Na$_3$-GTP, pH 7.3, 300 mOsm, resistances 4–7 MΩ. Coverslips containing hECNs were placed in the recording chamber and perfused using gravity feed with an extracellular solution composed of the following (in mM): 152 NaCl, 2.8 KCl, 10 HEPES, 2 CaCl$_2$, 10 glucose, pH 7.3, 320–330 mOsm. Recordings were made at 20–23°C. The liquid junction potential (LJP) was calculated to be $+14$ mV (JPCalc; Clampex). Perforated whole-cell recordings were performed using a gramicidin (50–100 μg/ml) supplemented patch-pipette solution containing the following (in mM): 145 KCl, 1 MgCl$_2$, 0.1 CaCl$_2$, 1 EGTA, 10 HEPES, pH 7.3, 320–330 mOsm; the LJP was calculated to be -4.3 mV. The progress of perforation in the voltage-clamp configuration was monitored by the development of capacitive transients. Abrupt rises in transients indicated membrane rupture to the whole-cell configuration and the experiment was terminated. Once perforation stability was established, series resistances were <40 MΩ.

Data analysis. Nonstationary fluctuation analysis of slowly rising whole-cell currents evoked by AMPA were used to estimate the AMPAR unitary single-channel current. The analysis of AC and DC currents was performed as described previously (Brown et al., 1998) with the exception that the AC-coupled signal was filtered with a 1–1200 Hz band-pass frequency. All other recordings were low-pass filtered online at 2 kHz and all recordings were digitized at 10 kHz and recorded to computer hard disk using the WinEDR V2.7.6 Electrophysiology Data Recorder (J. Dempster, University of Strathclyde, United Kingdom; www.strath.ac.uk/Departments/ PhysPharm/). [Cl$^-$]$_{INT}$ was calculated using the Nernst equation in which extracellular [Cl$^-$] was converted into activity using an activity coefficient.

Data are presented as mean $\pm$ SEM. The number of experimental replicates is denoted as n and N represents the number of *de novo* preparations of batches from which n is obtained.

Results

Developmental maturation of AMPARs in hECNs

Functional AMPAR expression was assessed, at weekly intervals, by the ability of AMPA (50 μM) to elicit whole-cell currents. With

time, hECNs displayed an increase in AMPAR-mediated current densities together with an increase in the proportion of hECNs that responded to application of AMPA. Five weeks after aNPC plate-down, ~90% of all cells gave currents (Fig. 1B) that could be blocked by CNQX. AMPARs are tetrameric assemblies of different combinations of GluA1, GluA2, GluA3, or GluA4 subunits. AMPAR composition in rodent and human excitatory cortical neurons is developmentally regulated; GluA1/GluA4-containing stoichiometry predominates in immature neurons, whereas mature neurons have an increased expression of GluA1 and GluA2 subunits (Monyer et al., 1991; Talos et al., 2006a, 2006b; Orlandi et al., 2011). We assessed relative AMPAR subunit mRNA expression levels at 2 and 5 weeks after aNPC plate-down by qRT-PCR (Fig. 1C) and found significant increases in the relative mRNA expression levels for each of the AMPAR subunits.

GluA2 subunits are RNA edited, resulting in a gene-encoded glutamine codon in the M2 reentrant loop region being replaced by an arginine codon in ~99% of mRNA transcripts (for review, see Wright and Vissel, 2012). Moreover, the biophysical properties of AMPARs are considerably influenced by the presence of edited GluA2 [GluA2(R)] subunits that give rise to AMPARs that possess low single-channel conductances, low Ca^{2+} permeability, and insensitivity to polyamine-mediated channel block (Traynelis et al., 2010). To assess whether AMPARs expressed by hECNs show a developmental increase in the proportion of receptors containing GluA2(R) subunits, we performed nonstationary fluctuation analysis to estimate the mean unitary conductance (γ) of AMPARs at weeks 2 and 5 after aNPC plate-down. Current-variance plots constructed from AC- and DC-coupled components of whole-cell AMPAR-mediated responses were used to estimate unitary conductances (Fig. 1D,E). Figure 1F illustrates that, for the ES1 cell line, the mean unitary conductance decreases at week 2 from 10.9 ± 1.0 pS ($n = 13$, $N = 2$) to 4.5 ± 0.4 pS at week 5 ($n = 12$, $N = 3$, $p < 0.001$, unpaired t test). Significant decreases in conductance over this same period were also observed in hECNs derived from a separate ES cell line (denoted ES2) and from two independent IPS cell lines (Fig. 1F). The factors that control the developmental increase in the expression of GluA2(R)-containing AMPARs remain largely unknown (Traynelis et al., 2010) and we found no evidence that this regulation is mediated by excitatory or inhibitory neurotransmitter action or is regulated by an activity-dependent process, because pharmacological blockade from weeks 1–5 of AMPAR, NMDAR, GABA_AR, and glycine receptors by CNQX (15 μM), D-AP5 (25 μM), bicuculline (100 μM), and strychnine (400 μM), respectively, and voltage-dependent Na^+ channels by TTX (1 μM) did not prevent the decrease in conductance that occurs between weeks 2 and 5 after aNPC differentiation (Fig. 1G). Furthermore, media supplements (see Materials and Methods) are not implicated in the reduction of conductance, because hECNs maintained in the absence of supplements displayed equivalent estimates of conductance at week 2 (12.7 $\pm$ 1.5; $n = 11$, $N = 3$) and week 5 (5.0 $\pm$ 1.1; $n = 5$, $N = 1$).

An increase in the proportion of AMPARs containing GluA2(R) subunits was confirmed in hECNs by assessing the polyamine sensitivity of AMPAR-mediated current to 1-naphthyl acetyl spermine (NASPM), a selective antagonist of GluA2(R)-lacking AMPARs (Koike et al., 1997). At week 2, NASPM (3 μM) strongly inhibited (77 $\pm$ 5%) AMPA-evoked steady-state whole-cell currents (Fig. 2A). The extent of this block is consistent with the expression of AMPARs that lack GluA2(R) subunits. At week 5, NASPM gave only modest inhibition (Fig. 2B,C). Overall, these data, together
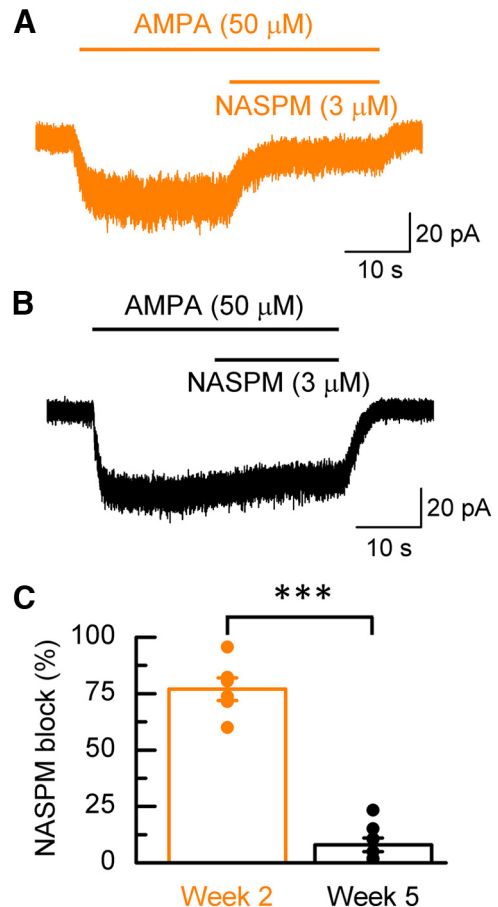
Figure 2. NASPM block. Example recordings from week 2 (**A**) and week 5 (**B**) neurons demonstrating NASPM inhibition of the steady-state current response evoked by AMPA. **C**, Mean percentage block of AMPA currents by NASPM. $n = 6–8$, $N = 2$, unpaired t test.

with a development switch in unitary conductance of AMPARs, are entirely consistent with a switch from a GluA2(R)-lacking to a GluA2(R)-containing AMPAR population.

hECNs show a developmental reduction in $[Cl^-]_{INT}$

Functional GABA_AR expression was assessed at weekly intervals by the ability of GABA (100 μM) to elicit whole-cell currents. The magnitude of steady-state GABA-evoked currents increased with increasing periods of culture and, after 4 weeks of differentiation, all cells responded to GABA (Fig. 3A) with robust currents that were blocked by picrotoxin.

Fast depolarizing actions of GABA on neural precursor cells and immature cortical neurons are well documented and are a consequence of higher $[Cl^-]_{INT}$ (~25 mM) due to the higher relative expression level of NKCC1 over KCC2 (Ben-Ari et al., 2007). In both rodent and human cortex, the postnatal expression levels of KCC2 increase (Dzhala et al., 2005), leading to a net extrusion of Cl^- from excitatory neurons and levels of $[Cl^-]_{INT}$ of 5–10 mM, which results in a net inward movement of Cl^- and a hyperpolarizing response in neurons at or near their resting membrane potentials (Blaesse et al., 2009). Using gramicidin-perforated current-clamp recording to prevent disruption of $[Cl^-]_{INT}$ (Kyrozis and Reichling, 1995), we assessed the nature of the GABA response in hECNs when held at a potential of −60 mV. After 1 week of culture after aNPC plate-down, GABA elicited a depolarizing response (Fig. 3B), whereas at later periods, the response was hyperpolarizing (Fig. 3C). To determine the
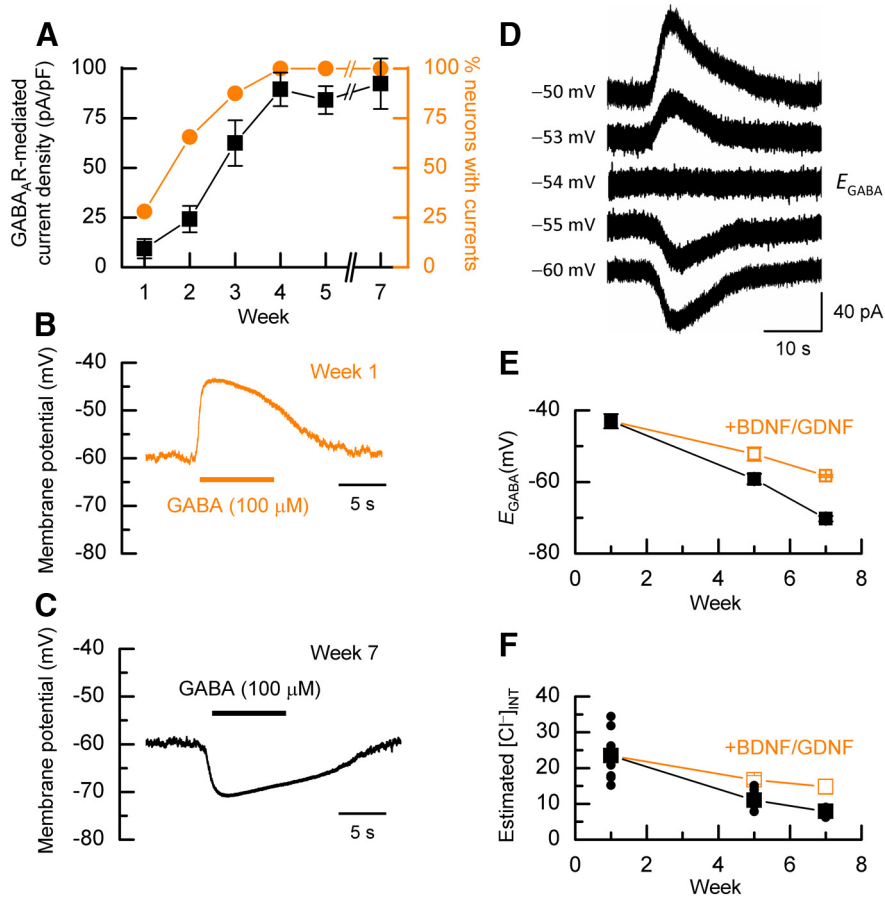
Figure 3. Determining $[Cl^-]_{INT}$. **A**, Weekly percentage response (orange) to GABA and the mean GABA-mediated current density (black; $n = 20–34$, $N = 1–4$). **B**, **C**, Example perforated current-clamp recordings, at -60 mV from week 1 (**B**) and week 7 (**C**) neurons in which either a depolarizing or hyperpolarizing response to GABA is observed. **D**, Representative voltage-clamp recordings used to determine E_{GABA}. **E**, The relationship between mean E_{GABA} in the absence ($n = 12–13$, $N = 2–3$) and presence of BDNF and GDNF ($n = 4–19$, $N = 1–3$). **F**, Mean $[Cl^-]_{INT}$ development. Data at week 7 were obtained in the presence of IGF1. $n = 12–13$, $N = 2–3$.

Figure 3F illustrates the estimated $[Cl^-]_{INT}$ derived using the Nernst equation at each of the time points studied in Figure 3E. At week 1, the mean $[Cl^-]_{INT}$ is 23.5 ± 1.9 mM and this decreases by week 7 to 7.9 ± 0.2 mM. In the presence of BDNF and GDNF, $[Cl^-]_{INT}$ remains elevated at weeks 5 and 7. A reduction in $[Cl^-]_{INT}$ was also observed in hECNs derived from other hPSC lines (Fig. 4A). The underlying regulation of native neuronal NKCC1/KCC2/$[Cl^-]_{INT}$ development is controversial (Ben-Ari et al., 2012). We have demonstrated that the reduction in $[Cl^-]_{INT}$ in hECNs cannot be prevented by pharmacological blockade, from weeks 1 to 7, of ion channels and neurotransmitter systems, as described previously for AMPAR development (Fig. 4B). The reduction of $[Cl^-]_{INT}$ in hECNs is therefore activity-independent. Finally, using qRT-PCR analysis, we examined whether hECNs displayed shifts in NKCC1/KCC2 mRNA transcript levels. At week 1, NKCC1 mRNA levels were 4.8-fold higher than that of KCC2, but by week 7, KCC2 mRNA levels were 3.1-fold higher than NKCC1 (Fig. 4C). Such findings are consistent with the change in the expression levels of NKCC1 and KCC2 that are observed in rodent neurons when $[Cl^-]_{INT}$ decreases during development (Blaesse et al., 2009). In addition, hECNs cultured in the presence of BDNF and GDNF, which resulted in a smaller fall in $[Cl^-]_{INT}$, exhibited smaller relative shifts in the expression of KCC2 mRNA to that of NKCC1.

reversal potential for GABA$_A$R-mediated responses (E_{GABA}), perforated voltage-clamp recordings were made from hECNs at various time points after aNPC differentiation. Figure 3D illustrates a series of GABA-activated current traces obtained from a week 5 hECNs and recorded at holding potentials that allowed E_{GABA} to be determined. Figure 3E summarizes the extent to which E_{GABA} changes with time in culture. At week 1, the mean E_{GABA} is -43.0 ± 2.0 mV ($n = 12$, $N = 3$) and becomes progressively more negative such that, at week 5, it is -59.2 ± 1.5 mV ($n = 11$, $N = 2$, $p < 0.001$). To examine the possibility that E_{GABA} could become more negative, we extended the culture period of hECNs to 7 weeks, which necessitated the inclusion of IGF1 in the culture media to improve cell viability (see Materials and Methods), and observed a further decrease in E_{GABA} to -70.3 ± 0.7 mV ($n = 13$, $N = 3$, $p < 0.001$). IGF1 was unlikely to have directly affected the change in E_{GABA} because hECNs at week 5 cultured in the presence of IGF1 did not show any change in E_{GABA} (-62.9 ± 2.3 mV; $n = 10$, $N = 2$). In these experiments, BDNF and GDNF were omitted because these neurotrophic factors have been reported to cause alterations in Cl^- transporter function and expression (Blaesse et al., 2009). Indeed, although E_{GABA} becomes more negative in the presence of BDNF and GDNF, it remains ~10 mV more positive than is observed for hECNs cultured in the absence of neurotrophic factors (Fig. 3E).

Discussion

We have demonstrated the ability of hECNs to functionally express mature GluA2(R)-containing AMPARs and exhibit a reduction in $[Cl^-]_{INT}$ to adult-like levels. Importantly for the interpretation of our results, differentiating aNPCs are likely to be the predominate cellular phenotype at early culture time points (weeks 1 and 2) and, by later time points ($\geq$week 4), the cultures are predominantly of hECN identity (Fig. 1A; Bilican et al., 2014).

We demonstrate that AMPAR single-channel conductance at weeks 2 and 5 significantly reduces from 10.9 to 4.5 pS in accordance with increased functional expression of the GluA2(R) subunit that confers a lower conductance to the AMPAR complex. Indeed, the conductance values at weeks 2 and 5 are directly comparable to conductance measurements of AMPAR-mediated events from rodent excitatory cortical neurons during a postnatal developmental period involving the upregulation of the GluA2(R) subunit (Brill and Huguenard, 2008). Furthermore, week 5 data correspond well to those of recombinantly expressed heteromeric GluA2(R)-containing AMPARs (Swanson et al., 1997). A GluA2(R)-lacking to GluA2(R)-containing switch in AMPAR subunits is confirmed by the observed high sensitivity of
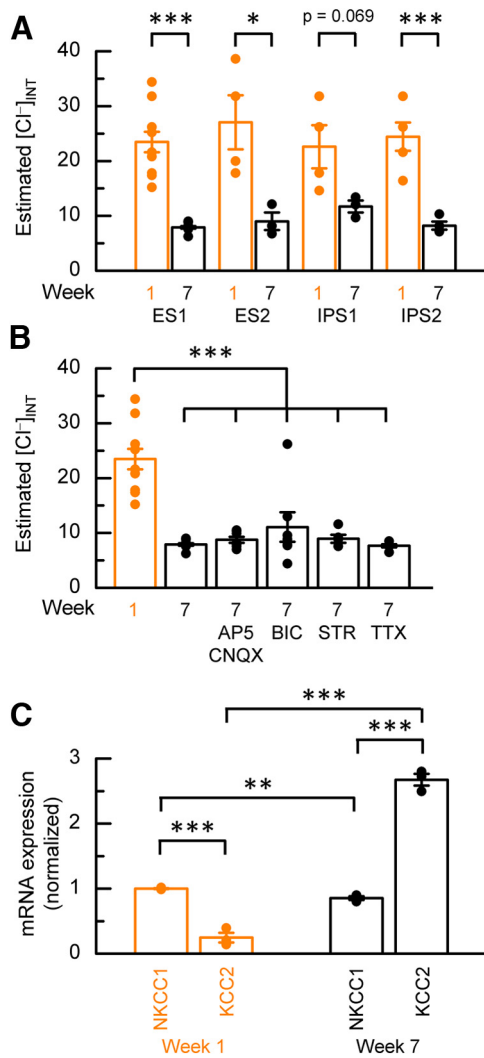
Figure 4. The maturation of [Cl$^-$]$_{INT}$. **A**, Decrease in mean [Cl$^-$]$_{INT}$ are observed in other hPSC lines. $n = 3–13$, $N = 1–3$, unpaired t test. **B**, The switch to low [Cl$^-$]$_{INT}$ is independent of neurotransmitter action and action potential driven activity. $n = 5–12$, $N = 2–3$, Kruskal–Wallis test with *post hoc* Dunn's test. **C**, Mean normalized mRNA fold expression data for Cl$^-$ transporter NKCC1 and KCC2 subunits as assessed by qRT-PCR. $n = 3$, $N = 2$, paired t test. Expression is normalized to week 1 NKCC1 data after normalizing to GAPDH.

AMPAR-mediated currents at week 2, but not at week 5, to GluA2(R)-lacking the AMPAR blocker NASPM.

The principal AMPAR composition in native cortical preparations has been described to develop from an immature GluA1/GluA4-containing to an adult GluA1/GluA2-containing AMPAR complex (Monyer et al., 1991; Talos et al., 2006a, 2006b; Orlandi et al., 2011). Our data are consistent with an upregulation of the GluA2 subunit from weeks 2 to 5, however, the mRNA data for hECNs also demonstrate an equivalent upregulation of the GluA4 subunit. Nevertheless, these data do not indicate the level of functional protein. At week 2, the cultures contain a mixture of neurons and aNPCs, so it is interesting that native primary human embryonic cortical NPCs express unedited forms of the GluA2 subunit [GluA2(Q)] and, upon neuronal differentiation, express the edited GluA2(R) subunit over an equivalent culture period (Whitney et al., 2008).

The underlying mechanism of this AMPAR subunit shift has not yet been described in native excitatory cortical neurons. Here, we demonstrate that the reduction of AMPAR conductance is not

prevented by antagonists of neurotransmitter ligand-gated ion channels and voltage-gated ion channels, indicating that the developmental upregulation of GluA2(R)-containing AMPARs is activity-independent. Indeed, it has been reported that NPC differentiation results in a large upregulation of the ADAR2 enzyme responsible for the editing of the GluA2 subunit Q/R site (Whitney et al., 2008).

We next investigated the regulation of [Cl$^-$]$_{INT}$. The understanding regarding the regulation, expression, and activity of Cl$^-$ transporters and [Cl$^-$]$_{INT}$ regulation is relevant to development and disease associated with GABA$_A$R (and other Cl$^-$ channel) function (Blaesse et al., 2009). Perforated-patch clamp measurements of E_{GABA} from weeks 1 to 7 show that [Cl$^-$]$_{INT}$ reduces from 24 to 8 mM. This is directly comparable to studies examining the maturation of [Cl$^-$]$_{INT}$ from NPCs to postnatal neurons in the rodent cortex (Owens et al., 1996; Yamada et al., 2004). In direct accordance with native mechanisms regulating [Cl$^-$]$_{INT}$, a reduction in [Cl$^-$]$_{INT}$ coincided with a switch in the relative mRNA expression levels of the Cl$^-$ transporters NKCC1 and KCC2 (Blaesse et al., 2009). This implies that the high [Cl$^-$]$_{INT}$ observed at week 1 is due to dominant NKCC1 activity and the low [Cl$^-$]$_{INT}$ observed at week 7 is a result of overriding KCC2-mediated Cl$^-$ extrusion.

To obtain a reduction in [Cl$^-$]$_{INT}$, hECNs had to be cultured for extended periods in the absence of BDNF and GDNF but with IGF supplementation. IGF1 was shown not to have an effect upon E_{GABA} in week 5 hECNs, but has previously been associated with an upregulation of KCC2 expression in rodent hippocampal neurons (Kelsch et al., 2001). The inclusion of BDNF and GDNF, however, appears to slow the developmental [Cl$^-$]$_{INT}$ reduction. Neurotrophic supplements are commonly used in hPSC-derived neuronal cultures with little regard for their potential impact on neuronal Cl$^-$ transporter function (Blaesse et al., 2009) and receptor densensitization (Frank et al., 1996). We thus advocate caution when using these agents, particularly for functional studies.

The mechanistic control of neuronal of [Cl$^-$]$_{INT}$ development has received considerable attention and specific reports of mechanisms of NKCC1 and KCC2 regulation have been controversial (Ben-Ari et al., 2012). The inability to prevent the reduction of [Cl$^-$]$_{INT}$ by chronic blockade of ion channel activity are in agreement with an activity-independent mechanism in hECNs that has been observed in native neuronal preparations (Ben-Ari et al., 2007).

In summary, we show the ability of hECNs to functionally express mature GluA2(R)-containing AMPARs. This enables investigation into disease mechanisms that may affect the editing at the Q/R site. Furthermore, the ability of hECNs to exhibit a reduction in [Cl$^-$]$_{INT}$ to adult levels enables homeostatic and disease studies that potentially affect Cl$^-$ transporter function.

References

Ben-Ari Y, Gaiarsa JL, Tyzio R, Khazipov R (2007) GABA: a pioneer transmitter that excites immature neurons and generates primitive oscillations. Physiol Rev 87:1215–1284. CrossRef Medline

Ben-Ari Y, Woodin MA, Sernagor E, Cancedda L, Vinay L, Rivera C, Legendre P, Luhmann HJ, Bordey A, Wenner P, Fukuda A, van den Pol AN, Gaiarsa JL, Cherubini E (2012) Refuting the challenges of the developmental shift of polarity of GABA actions: GABA more exciting than ever! Front Cell Neurosci 6:35. CrossRef Medline

Bilican B, Serio A, Barmada SJ, Nishimura AL, Sullivan GJ, Carrasco M, Phatnani HP, Puddifoot CA, Story D, Fletcher J, Park IH, Friedman BA, Daley GQ, Wyllie DJ, Hardingham GE, Wilmut I, Finkbeiner S, Maniatis T, Shaw CE, Chandran S (2012) Mutant induced pluripotent stem cell lines recapitulate aspects of TDP-43 proteinopathies and reveal cell-

specific vulnerability. Proc Natl Acad Sci U S A 109:5803–5808. CrossRef Medline

Bilican B, Livesey MR, Haghi G, Qiu J, Burr K, Siller R, Hardingham GE, Wyllie DJ, Chandran S (2014) Physiological oxygen levels and EGF withdrawal are required for scalable generation of functional cortical neurones from human pluripotent stem cells. Plos One 9:e85932. CrossRef Medline

Blaesse P, Airaksinen MS, Rivera C, Kaila K (2009) Cation-chloride cotransporters and neuronal function. Neuron 61:820–838. CrossRef Medline

Brill J, Huguenard JR (2008) Sequential changes in AMPA receptor targeting in the developing neocortical excitatory circuit. J Neurosci 28:13918–13928. CrossRef Medline

Brown AM, Hope AG, Lambert JJ, Peters JA (1998) Ion permeation and conduction in a human recombinant 5-HT3 receptor subunit (h5-HT3A). J Physiol 507:653–665. CrossRef Medline

Dzhala VI, Talos DM, Sdrulla DA, Brumback AC, Mathews GC, Benke TA, Delpire E, Jensen FE, Staley KJ (2005) NKCC1 transporter facilitates seizures in the developing brain. Nat Med 11:1205–1213. CrossRef Medline

Espuny-Camacho I, Michelsen KA, Gall D, Linaro D, Hasche A, Bonnefont J, Bali C, Orduz D, Bilheu A, Herpoel A, Lambert N, Gaspard N, Péron S, Schiffmann SN, Giugliano M, Gaillard A, Vanderhaeghen P (2013) Pyramidal neurons derived from human pluripotent stem cells integrate efficiently into mouse brain circuits in vivo. Neuron 77:440–456. CrossRef Medline

Frank L, Ventimiglia R, Anderson K, Lindsay RM, Rudge JS (1996) BDNF down-regulates neurotrophin responsiveness, TrkB protein and TrkB mRNA levels in cultured rat hippocampal neurons. Eur J Neurosci 8:1220–1230. CrossRef Medline

Hansen DV, Rubenstein JL, Kriegstein AR (2011) Deriving excitatory neurons of the neocortex from pluripotent stem cells. Neuron 70:645–660. CrossRef Medline

Johnson MA, Weick JP, Pearce RA, Zhang SC (2007) Functional neural development from human embryonic stem cells: accelerated synaptic activity via astrocyte coculture. J Neurosci 27:3069–3077. CrossRef Medline

Kelsch W, Hormuzdi S, Straube E, Lewen A, Monyer H, Misgeld U (2001) Insulin-like growth factor 1 and a cytosolic tyrosine kinase activate chloride outward transport during maturation of hippocampal neurons. J Neurosci 21:8339–8347. Medline

Koike M, Iino M, Ozawa S (1997) Blocking effect of 1-naphthyl acetyl spermine on Ca(2+)-permeable AMPA receptors in cultured rat hippocampal neurons. Neurosci Res 29:27–36. CrossRef Medline

Kyrozis A, Reichling DB (1995) Perforated-patch recording with gramicidin avoids artifactual changes in intracellular chloride concentration. J Neurosci Methods 57:27–35. CrossRef Medline

Monyer H, Seeburg PH, Wisden W (1991) Glutamate-operated channels: developmentally early and mature forms arise by alternative splicing. Neuron 6:799–810. CrossRef Medline

Orlandi C, La Via L, Bonini D, Mora C, Russo I, Barbon A, Barlati S (2011) AMPA receptor regulation at the mRNA and protein level in rat primary cortical cultures. Plos One 6:e25350. CrossRef Medline

Owens DF, Boyce LH, Davis MB, Kriegstein AR (1996) Excitatory GABA responses in embryonic and neonatal cortical slices demonstrated by gramicidin perforated-patch recordings and calcium imaging. J Neurosci 16:6414–6423. Medline

Sandoe J, Eggan K (2013) Opportunities and challenges of pluripotent stem cell neurodegenerative disease models. Nat Neurosci 16:780–789. CrossRef Medline

Shi Y, Kirwan P, Smith J, Robinson HP, Livesey FJ (2012) Human cerebral cortex development from pluripotent stem cells to functional excitatory synapses. Nat Neurosci 15:477–486, S1. CrossRef Medline

Swanson GT, Kamboj SK, Cull-Candy SG (1997) Single-channel properties of recombinant AMPA receptors depend on RNA editing, splice variation, and subunit composition. J Neurosci 17:58–69. Medline

Talos DM, Fishman RE, Park H, Folkerth RD, Follett PL, Volpe JJ, Jensen FE (2006a) Developmental regulation of alpha-amino-3-hydroxy-5-methyl-4-isoxazole-propionic acid receptor subunit expression in forebrain and relationship to regional susceptibility to hypoxic/ischemic injury. I. Rodent cerebral white matter and cortex. J Comp Neurol 497:42–60. CrossRef Medline

Talos DM, Follett PL, Folkerth RD, Fishman RE, Trachtenberg FL, Volpe JJ, Jensen FE (2006b) Developmental regulation of alpha-amino-3-hydroxy-5-methyl-4-isoxazole-propionic acid receptor subunit expression in forebrain and relationship to regional susceptibility to hypoxic/ischemic injury. II. Human cerebral white matter and cortex. J Comp Neurol 497:61–77. CrossRef Medline

Traynelis SF, Wollmuth LP, McBain CJ, Menniti FS, Vance KM, Ogden KK, Hansen KB, Yuan H, Myers SJ, Dingledine R (2010) Glutamate receptor ion channels: structure, regulation, and function. Pharmacol Rev 62:405–496. CrossRef Medline

Whitney NP, Peng H, Erdmann NB, Tian C, Monaghan DT, Zheng JC (2008) Calcium-permeable AMPA receptors containing Q/R-unedited GluR2 direct human neural progenitor cell differentiation to neurons. FASEB J 22:2888–2900. CrossRef Medline

Wright A, Vissel B (2012) The essential role of AMPA receptor GluR2 subunit RNA editing in the normal and diseased brain. Front Mol Neurosci 5:34. CrossRef Medline

Yamada J, Okabe A, Toyoda H, Kilb W, Luhmann HJ, Fukuda A (2004) Cl⁻ uptake promoting depolarizing GABA actions in immature rat neocortical neurones is mediated by NKCC1. J Physiol 557:829–841. CrossRef Medline

Yang N, Ng YH, Pang ZP, Südhof TC, Wernig M (2011) Induced neuronal cells: how to make and define a neuron. Cell Stem Cell 9:517–525. CrossRef Medline

Zeng H, Guo M, Martins-Taylor K, Wang X, Zhang Z, Park JW, Zhan S, Kronenberg MS, Lichtler A, Liu HX, Chen FP, Yue L, Li XJ, Xu RH (2010) Specification of region-specific neurons including forebrain glutamatergic neurons from human induced pluripotent stem cells. Plos One 5:e11853. CrossRef Medline